Arch Appl Mech (2012) 82:937–948
DOI 10.1007/s00419-011-0602-4

ORIGINAL

H. H. Sherief · M. S. Faltas · E. A. Ashmawy

Stokes flow between two confocal rotating spheroids with slip

Received: 20 July 2011 / Accepted: 7 December 2011 / Published online: 20 December 2011

Abstract The steady axisymmetric flow problem of a viscous fluid confined between two confocal spheroids that are rotating about their axis of revolution with different angular velocities is considered. A linear slip, of Basset type, boundary condition on both surfaces of the spheroidal particle and the container is used. Under the Stokesian assumption, a general solution is constructed from the superposition of basic solutions in prolate and oblate spheroidal coordinates. The boundary conditions on the particle's surface and spheroidal container are satisfied by a collocation technique. The torque exerted on the spheroidal particle by the fluid is evaluated with good convergence for various values of the slip parameters, the relative angular velocity and aspect ratios of the spheroids. The limiting case of no-slip is in good agreement with the available values in the literature.

Keywords Rotational motion · Stokes flow · Prolate spheroid · Oblate spheroid · Slip condition

1 Introduction

The properties of confined fluids in a continuous medium at low Reynolds number have continued to receive much attention from researchers. In real situations of Stokes flow problems, particles or droplets are not isolated, and the surrounding fluid is externally bounded by solid walls. Thus, it is important to determine whether the presence of neighboring boundaries significantly affects the motion of a particle or droplet. The system of a particle moving inside a cavity can be taken as an idealized model for the capture of particles in filters composed of connecting pores of spherical or non-spherical shapes. The hydrodynamic interaction between the particle and the cavity wall determines the deposition behavior of the particle toward the wall and thus relates closely to the capture efficiency of the filter [1]. Problems of the hydrodynamic interactions between two or more particles and between particles and boundaries have been treated extensively in the past [2,3]. Among various rotating fluid systems, the motion of a viscous fluid contained between two concentric rotating spheres is of specific interest in both engineering design and geophysics because of its wide application in different fields, for example, centrifuges, fluid gyroscopes [4], and colloidal science [2,5–9].

Landau and Lifshitz [10] discussed the slow motion of fluid contained in the space between two concentric spheres. Munsun and Joseph [11] also investigated the problem of steady motion of a viscous fluid contained between two concentric spheres which rotate about a common axis with different angular velocities and allowing for the inertia term. For the rotating bodies, it is important to evaluate the couple experienced on bodies by the fluid. The value of this couple is needed in designing and calibrating viscometers, and better predictions of couple are essential in order to improve the accuracy of viscosity measurements [12].

One of the basic concepts of fluid mechanics is the no-slip boundary condition, i.e., assuming that the layer of fluid next to a solid surface moves with the local velocity of the surface. This no-slip boundary condition has

H. H. Sherief · M. S. Faltas · E. A. Ashmawy (✉)
Department of Mathematics, Faculty of Science, Alexandria University, Alexandria, Egypt
E-mail: emad_ashm@yahoo.com

been applied successfully to model many macroscopic experiments but has no microscopic justification. There exist situations in which the no-slip boundary condition leads to singular or unrealistic behavior, e.g., [13–23]. In recent years, there has been an increased interest in determining the appropriate boundary conditions for the flow of Newtonian fluids in confined geometries. In fact, nearly 200 years ago, Navier [24] proposed a general boundary condition that permits the possibility of fluid slip at a solid boundary. This condition assumes that the tangential velocity of the fluid relative to the solid at a point on its surface is proportional to the tangential stress acting at that point. Fluid slip has been observed experimentally in micro- and nano-scale flow devices by several investigators, e.g., [25–28]. Neto et al. [29] provided an excellent review of experimental studies regarding the phenomenon of slip of Newtonian fluids at solid interface.

In recent years, there has been an increased interest in using the slip boundary condition to solve flow problems in viscous, micropolar, and microstretch fluids, e.g., [30–36]. Loyalka and Griffin [37] have studied numerically the rotation of non-spherical axisymmetric particles in the slip regime using the Green's function technique to determine the local stresses and torques on single particles. Previous work on the rotation of single, spherical, and non-spherical particles has been reviewed by Williams and Loyalka [38]. Recently Chang and Keh [39] investigated, using spheroidal coordinates, the problem of rotation of a slip spheroidal particle about its axis of revolution. They evaluated the torque exerted on the spheroidal particle by the fluid for various values of the slip parameter and aspect ratio of the particle. More recently, Ashmawy [40] studied the rotational motion of an arbitrary axisymmetric slip particle in a viscous fluid using a combined analytical–numerical technique. Numerical results are obtained for the special cases of prolate spheroid and Cassini oval particles. It should be noted here that it is a matter of difficulty to obtain analytical solution for the problem of rotation of non-spherical particle allowing the fluid to slip at the surface of the particle.

The boundary collocation technique has been used by many authors to solve flow problems in viscous fluids. Gluckman et al. [41] developed truncated series boundary collocation method to study the unbounded axisymmetric multispherical Stokes flow. The theoretically predicated drag results are in good agreement with experimentally measured values. Later, Leichtberg et al. [42] extended the work of Gluckman et al. [41] to bounded flows for coaxial chains of spheres in a tube. Ganatos et al. [43,44] modified the collocation series solution techniques to investigate the Stokes flow of perpendicular and parallel motion of a sphere between two parallel plane boundaries. The collocation method has been also used to treat the axisymmetric slip flow problems, e.g., [45–47]. It is also used to solve micropolar fluid flow, e.g., [35,48].

This paper investigates Stokes flow of an incompressible viscous fluid between two confocal spheroids which are rotating steadily about their axis of revolution with different angular velocities. The fluid is allowed to slip frictionally at the surface of a prolate or oblate spheroidal particle and at the surface of its container. A combined analytical-numerical method with the boundary collocation technique has been used to solve the Stokes equations for the fluid flow field. The rotational torque coefficient is obtained with good convergence for various parameters considered.

2 Mathematical formulation

We consider here the steady motion of an incompressible viscous fluid of viscosity μ that fills the gap between two confocal spheroids which are rotating about their axis of revolution, as shown in Fig. 1. The angular velocity of the spheroidal particle is $\omega_1\vec{e}_z$ whereas for the container is $\omega_2\vec{e}_z$, where $\vec{e}_z$ is the unit vector in the positive z-direction. The fluid is allowed to slip frictionally at particle and container surfaces.

It is convenient to use both the circular cylindrical coordinates (ρ, ϕ, z) and the bifocal coordinates (ξ, η, ϕ) with the origin of coordinates located at the center of the container. Spheroidal particles can be either prolate or oblate. Using a simple transformation, we can obtain the results for the oblate particles from those for the prolate spheroidal particles. Therefore, we begin by investigating the case of prolate spheroidal particles only. Let the surface of the spheroidal particle S_p is represented by $\xi = \xi_1$ or by

$$\frac{z^2}{a_1^2} + \frac{\rho^2}{b_1^2} = 1, \tag{2.1}$$

and the surface of its confocal container S_c is represented by $\xi = \xi_2$ or by

$$\frac{z^2}{a_2^2} + \frac{\rho^2}{b_2^2} = 1, \tag{2.2}$$

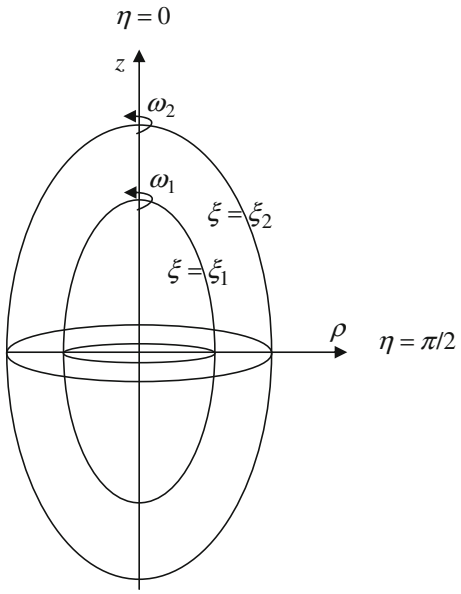

Fig. 1 Geometrical sketch for rotating confocal spheroids

where a_1, a_2 are the half-lengths, along the axis of revolution, and b_1, b_2 are the equatorial radii of the particle and container, respectively. It is appropriate to use the semi-focal length $c = \sqrt{a_i^2 - b_i^2}$ as a characteristic length. The cylindrical coordinates are related to the prolate spheroidal ones through the equations

$$z = c\cosh\xi\cos\eta, \quad \rho = c\sinh\xi\sin\eta, \tag{2.3}$$

where $0 \le \xi < \infty, \quad 0 \le \eta \le \pi$.
Therefore

$$a_i = c\cosh\xi_i, \quad b_i = c\sinh\xi_i, \quad (i = 1, 2) \tag{2.4}$$

It is convenient to introduce the following independent variables [2]:

$$\tau = \cosh\xi, \quad \zeta = \cos\eta, \quad |\tau| > 1, \quad -1 \le \zeta \le 1. \tag{2.5}$$

At this point, the surfaces of the spheroidal particle S_p and the container S_c are represented, respectively, by $\tau_i = \frac{a_i}{c}$, $(i = 1, 2)$.

Under the Stokesian approximation, the fluid flow is governed by the equations

$$\nabla \cdot \vec{q} = 0, \tag{2.6}$$

$$\nabla p - \mu\nabla^2\vec{q} = 0, \tag{2.7}$$

where $\vec{q}$ is the velocity field and p is the dynamic pressure distribution. The flow is axially symmetric and all physical quantities are independent of ϕ; therefore,

$$\vec{q} = q_\phi\vec{e}_\phi, \tag{2.8}$$

where $\vec{e}_\phi$ is a unit vector perpendicular to the meridian planes ϕ = constant. Under these circumstances, Eq. (2.6) is satisfied automatically, the dynamic pressure keeps constant everywhere in the fluid region, and the velocity component q_ϕ satisfies the following equation:

$$E^2(\rho q_\phi) = 0, \tag{2.9}$$

where the operator E^2 is given by

$$E^2 = \frac{1}{c(\tau^2 - \zeta^2)}\left[(\tau^2 - 1)\frac{\partial^2}{\partial\tau^2} + (1 - \zeta^2)\frac{\partial^2}{\partial\zeta^2}\right]. \tag{2.10}$$

To complete the formulation of the problem, the boundary condition has to be specified. At the surfaces of the spheroidal particle and container, we shall assume linear slip boundary condition of Basset type [49] which states that the relative tangential velocity of the fluid at the solid surface is proportional to the local shear rate. Therefore,

$$q_\phi = \rho\omega_1 + \frac{1}{\beta_1} t_{\tau\phi} \quad \text{on} \quad S_p : \tau = \tau_1, \tag{2.11}$$

$$q_\phi = \rho\omega_2 - \frac{1}{\beta_2} t_{\tau\phi} \quad \text{on} \quad S_c : \tau = \tau_2, \tag{2.12}$$

where $t_{\tau\phi}$ is the fluid shear stress, which can be expressed as

$$t_{\tau\phi} = \frac{\mu\sqrt{\tau^2-1}}{c\sqrt{\tau^2-\zeta^2}} \left[\frac{\partial q_\phi}{\partial \tau} - \frac{\tau}{\tau^2-1} q_\phi \right], \tag{2.13}$$

and the constant, β_i, termed as the coefficient of sliding friction. This coefficient is a measure of the degree of tangential slip existing between the fluid and solid at its surface. It is assumed to depend only on the nature of the fluid and solid surface. In the limiting case of $\beta_i = 0$, there is a perfect slip, while the standard no-slip boundary condition for solids is obtained by letting $\beta_i \to \infty$.

3 Method of solution

Substituting (2.10) into Eq. (2.9), we get

$$\left(\tau^2-1\right) \frac{\partial^2 q_\phi}{\partial \tau^2} + 2\tau \frac{\partial q_\phi}{\partial \tau} - \frac{q_\phi}{\tau^2-1} + \left(1-\zeta^2\right) \frac{\partial^2 q_\phi}{\partial \zeta^2} - 2\zeta \frac{\partial q_\phi}{\partial \zeta} - \frac{q_\phi}{1-\zeta^2} = 0. \tag{3.1}$$

Putting $q_\phi = f(\tau)g(\zeta)$, we obtain the following ordinary differential equations

$$\left(1-\tau^2\right) f'' - 2\tau f' + \left[n(n+1) - \frac{1}{1-\tau^2} \right] f = 0, \tag{3.2}$$

$$\left(1-\zeta^2\right) g'' - 2\zeta g' + \left[n(n+1) - \frac{1}{1-\zeta^2} \right] g = 0, \tag{3.3}$$

where $n(n+1)$ is the separation constant. Therefore, after omitting the irregular terms, a general solution of Eq. (3.1) in the fluid region $\tau_1 < \tau < \tau_2, 0 \le \eta \le \pi$ is given by [50]

$$q_\phi = \omega_1 c \sum_{k=1}^{\infty} \left[A_{2k-1} Q^1_{2k-1}(\tau) + B_{2k-1} P^1_{2k-1}(\tau) \right] P^1_{2k-1}(\zeta), \tag{3.4}$$

where P^1_n and Q^1_n are the associated Legendre polynomials of the first and second kinds, respectively, of order n and degree 1, and A_n, B_n are unknown coefficients. Note that, since q_ϕ is symmetric about the equatorial plane $z = 0$, we keep only the odd terms in the series solution (3.4).
Substitute from (3.4) into (2.13) and using the identities

$$\frac{\mathrm{d}}{\mathrm{d}\tau} P^1_n(\tau) = \frac{1}{\tau^2-1} \left[n\tau P^1_n(\tau) - (n+1) P^1_{n-1}(\tau) \right]$$

$$\frac{\mathrm{d}}{\mathrm{d}\tau} Q^1_n(\tau) = \frac{1}{\tau^2-1} \left[n\tau Q^1_n(\tau) - (n+1) Q^1_{n-1}(\tau) \right]$$

the shear stress is given by

$$t_{\tau\phi} = \frac{\mu\omega_1}{\sqrt{\tau^2-\zeta^2}} \sum_{k=1}^{\infty} \left[A_{2k-1} F_{2k-1}(\tau) + B_{2k-1} G_{2k-1}(\tau) \right] P^1_{2k-1}(\zeta), \tag{3.5}$$

where

$$F_n(\tau) = \frac{1}{\sqrt{\tau^2-1}}\left((n-1)\tau Q_n^1(\tau) - (n+1)Q_{n-1}^1(\tau)\right),$$
$$G_n(\tau) = \frac{1}{\sqrt{\tau^2-1}}\left((n-1)\tau P_n^1(\tau) - (n+1)P_{n-1}^1(\tau)\right).$$

From (2.3) and (2.5), we have

$$\rho = c\sqrt{\tau^2-1}\sqrt{1-\zeta^2}. \tag{3.6}$$

Substituting the relations (3.4), (3.5), and (3.6) into the boundary conditions (2.11) and (2.12), we get

$$\begin{aligned}\sum_{k=1}^{\infty}\Bigg[A_{2k-1}\left(Q_{2k-1}^1(\tau_1) - \tfrac{\mu}{c\beta_1}\tfrac{\sqrt{\tau_1^2-1}}{\sqrt{\tau_1^2-\zeta^2}}F_{2k-1}(\tau_1)\right)\\ + B_{2k-1}\left(P_{2k-1}^1(\tau_1) - \tfrac{\mu}{c\beta_1}\tfrac{\sqrt{\tau_1^2-1}}{\sqrt{\tau_1^2-\zeta^2}}G_{2k-1}(\tau_1)\right)\Bigg]P_{2k-1}^1(\zeta) = \sqrt{\tau_1^2-1}\sqrt{1-\zeta^2},\end{aligned} \tag{3.7}$$

$$\begin{aligned}\sum_{k=1}^{\infty}\Bigg[A_{2k-1}\left(Q_{2k-1}^1(\tau_2) + \tfrac{\mu}{c\beta_2}\tfrac{\sqrt{\tau_2^2-1}}{\sqrt{\tau_2^2-\zeta^2}}F_{2k-1}(\tau_2)\right)\\ + B_{2k-1}\left(P_{2k-1}^1(\tau_2) + \tfrac{\mu}{c\beta_2}\tfrac{\sqrt{\tau_2^2-1}}{\sqrt{\tau_2^2-\zeta^2}}G_{2k-1}(\tau_2)\right)\Bigg]P_{2k-1}^1(\zeta) = \omega\sqrt{\tau_2^2-1}\sqrt{1-\zeta^2},\end{aligned} \tag{3.8}$$

where $\omega = \omega_2/\omega_1$ is the relative angular velocity of the spheroidal container. To determine the fluid velocity, the boundary conditions (3.7) and (3.8) should be satisfied exactly along the surface of spheroidal particle and the container surface. This would result in an infinite linear system of algebraic equations for an infinite number of unknown coefficients, which cannot be solved. This difficulty can be overcome by the use of a multipole collocation technique [41–44]. It requires first that the infinite series be truncated after a certain number of terms N (say) so that the number of the unknown coefficients becomes finite. Then, sufficient points on each of the particle surface and container surface are selected as collocation points, where the boundary conditions are enforced. Solving these equations (numerically) subsequently enables one to determine the flow field. In general, more boundary collocation points are required to attain a given accuracy when the axis ratio $\tau_2/\tau_1 = a_2/a_1$of container-to-particle is close to unity. As N tends to infinity, we get the exact solution.

3.1 The torque

The hydrodynamic torque (in the $z-$direction) exerted on the rotating spheroidal particle by the fluid, obtained from the moment of the stress about the axis of rotation, is given by

$$T = \int_{S_p}\vec{r}\wedge(\vec{n}\cdot\boldsymbol{t})\cdot\vec{k}\,\mathrm{d}S, \tag{3.9}$$

where

$$\vec{r} = \frac{c}{\sqrt{\tau_1^2-\zeta^2}}\left[\tau\sqrt{\tau_1^2-1}\vec{e}_\xi - \zeta\sqrt{\zeta^2-1}\vec{e}_\eta\right],$$

also, $\vec{n} = \vec{e}_\xi$ and $\vec{k}$ is the unit vector in the direction of the axis of rotation, $\boldsymbol{t}$ is the stress tensor, and the integral is taken over the boundary of the particle's surface; therefore,

$$T = 2\pi c^3\int_{-1}^{1} t_{\tau\phi}\left(\tau_1^2-1\right)\sqrt{\zeta^2-1}\sqrt{\tau_1^2-\zeta^2}\,\mathrm{d}\zeta, \tag{3.10}$$

Substitute for $t_{\tau\phi}$ from (3.5) and using the orthogonality relation of $P_n^1(\zeta)$, we obtain

$$T = -\frac{16}{3}\pi\mu c^3\omega_1 A_1. \tag{3.11}$$

The above expression shows that only the lowest-order coefficient A_1 contributes to the hydrodynamic torque acting on the particle. This leading coefficient normally is the most accurate (fastest convergent) result obtainable from the boundary collocation technique [39].

For the classical case of no-slip, we take the limit as $\beta_1 \to \infty$ and $\beta_2 \to \infty$ in Eqs. (3.7) and (3.8) to get

$$\sum_{k=1}^{\infty}\left[A_{2k-1}\left(Q_{2k-1}^1(\tau_1)\right) + B_{2k-1}\left(P_{2k-1}^1(\tau_1)\right)\right]P_{2k-1}^1(\zeta) = \sqrt{\tau_1^2-1}\sqrt{1-\zeta^2}, \tag{3.12}$$

$$\sum_{k=1}^{\infty}\left[A_{2k-1}\left(Q_{2k-1}^1(\tau_2)\right) + B_{2k-1}\left(P_{2k-1}^1(\tau_2)\right)\right]P_{2k-1}^1(\zeta) = \omega\sqrt{\tau_2^2-1}\sqrt{1-\zeta^2}, \tag{3.13}$$

Since $P_1^1(\zeta) = \sqrt{1-\zeta^2}$, equating the coefficients of $P_1^1(\zeta)$ in both sides of Eqs. (3.12), (3.13), we obtain

$$A_1 Q_1^1(\tau_1) + B_1 P_1^1(\tau_1) = \sqrt{\tau_1^2-1}, \tag{3.14}$$

$$A_1 Q_1^1(\tau_2) + B_1 P_1^1(\tau_2) = \frac{\omega_2}{\omega_1}\sqrt{\tau_2^2-1}. \tag{3.15}$$

Solving the above linear system and substituting into Eq. (3.11), we get after some straight forward simplifications an exact formula for the hydrodynamic torque acting on the surface of the spheroid in the form

$$T = \frac{16}{3}\pi\mu c^3\frac{(\omega_1-\omega_2)(\tau_1^2-1)(\tau_2^2-1)}{(\tau_1^2-1)(\tau_2^2-1)(\coth^{-1}\tau_2-\coth^{-1}\tau_1)+(\tau_2-\tau_1)(\tau_2\tau_1+1)}. \tag{3.16}$$

For spheroidal particle rotating with angular velocity ω_1 in a stationary container, the expression (3.16) reduces to

$$T = \frac{16}{3}\pi\mu\omega_1 c^3\frac{(\tau_1^2-1)(\tau_2^2-1)}{(\tau_1^2-1)(\tau_2^2-1)(\coth^{-1}\tau_2-\coth^{-1}\tau_1)+(\tau_2-\tau_1)(\tau_2\tau_1+1)}. \tag{3.17}$$

The torque experienced by the fluid on a spheroidal particle rotating, with an angular velocity ω_1 about its axis of revolution, in an unbounded fluid for the case of no-slip can be obtained from (3.17) by letting $\tau_2 \to \infty$. So we get

$$T = \frac{8}{3}\pi\mu\omega_1 b_1^3\left[\sqrt{\tau_1^2-1}\left(\tau_1 - \left(\tau_1^2-1\right)\coth^{-1}\tau_1\right)\right]^{-1}, \tag{3.18}$$

where $b_1 = c\sqrt{\tau_1^2-1}$.

This latter relation is in agreement with that of Jeffery [50].

4 Numerical results

The system of linear algebraic equations to be solved for the coefficients A_n, B_n using the boundary collocation technique is constructed from Eqs. (3.7) to (3.8). When specifying the Npoints along the quarter-elliptic generating arc of the spheroidal particle and its container where the boundary condition (3.7) and (3.8) are to be exactly satisfied, the first point that should be taken is $\eta = \pi/2(\zeta = 0)$, since this point defines the projected area of the particle normal to its axis of revolution. This point together with the point $\eta = 0(\zeta = 1)$ are singular points for the collocation method, so they need special considerations. A numerical examination of the system of linear algebraic equations in the truncated form shows that the coefficient matrix becomes singular if these points are used. To overcome this difficulty, these points are replaced by closely adjacent

points $\eta = \varepsilon$ and $\eta = \pi/2 - \varepsilon$. Additional points along the boundary are selected to divide the quarter-elliptic arc of the spheroid into segments into equal angles.

We present here, the collocation solutions of the normalized torque, $T_1/8\pi\mu c^3\omega_1$ experienced by the fluid on the slip spheroidal particle. Calculations are made for equal slip parameters on both of the spheroidal particle and the container and for various values of the following parameters:

(a) The axis ratio,
(b) The slip coefficient,
(c) The relative angular velocity.

The results are shown in Tables 1, 2 and in Figs. 2, 3 for prolate particle and in Tables 3, 4 and Figs. 4, 5 for oblate particle. It is observed that, in general, the magnitude of the normalized torque increases with the increase

Table 1 Normalized torque acting on the prolate spheroid $\xi = \xi_1$ with $\tau_2/\tau_1 = 2$

ω_2/ω_1	N	$T_1/8\pi\mu c^3\omega_1$				
		$c\beta/\mu = 0.01$	$c\beta/\mu = 0.1$	$c\beta/\mu = 1.0$	$c\beta/\mu = 10.0$	$c\beta/\mu = \infty$
−1.5	8	0.000794	0.007820	0.067713	0.290027	0.458716
	9	0.000794	0.007820	0.067713	0.290026	0.458716
0.0	8	0.000318	0.003128	0.027085	0.116011	0.183486
	9	0.000318	0.003128	0.027085	0.116011	0.183486
1.5	8	−0.000159	−0.001564	−0.013543	−0.058005	−0.091743
	9	−0.000159	−0.001564	−0.013543	−0.058005	−0.091743
2.0	8	−0.000318	−0.003128	−0.027085	−0.116011	−0.183486
	9	−0.000318	−0.003128	−0.027085	−0.116011	−0.183486
5.0	8	−0.001271	−0.012512	−0.108341	−0.464043	−0.733945
	9	−0.001271	−0.012512	−0.108341	−0.464042	−0.733945

Table 2 Normalized torque acting on the prolate spheroid $\xi = \xi_1$ with $\omega_2/\omega_1 = 2$

τ_2/τ_1	N	$T_1/8\pi\mu c^3\omega_1$				
		$c\beta/\mu = 0.01$	$c\beta/\mu = 0.1$	$c\beta/\mu = 1.0$	$c\beta/\mu = 10.0$	$c\beta/\mu = \infty$
1.1	7	−0.000252	−0.002497	−0.023161	−0.134686	−0.291700
	8	−0.000252	−0.002497	−0.023161	−0.134688	−0.291700
1.2	7	−0.000285	−0.002820	−0.025342	−0.126233	−0.227662
	8	−0.000285	−0.002820	−0.025342	−0.126234	−0.227662
1.5	7	−0.000311	−0.003068	−0.026801	−0.118681	−0.192645
	8	−0.000311	−0.003068	−0.026801	−0.118683	−0.192645
2.0	7	−0.000318	−0.003128	−0.027085	−0.116010	−0.183486
	8	−0.000318	−0.003128	−0.027085	−0.116011	−0.183486
10.0	7	−0.000320	−0.003145	−0.027130	−0.114720	−0.179437
	8	−0.000320	−0.003145	−0.027131	−0.114722	−0.179437

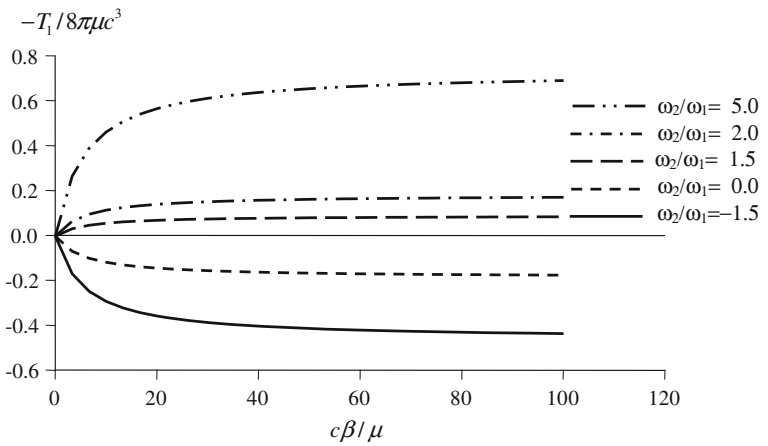

Fig. 2 Normalized torque acting on the prolate spheroid $\xi = \xi_1$ with $\tau_2/\tau_1 = 2$

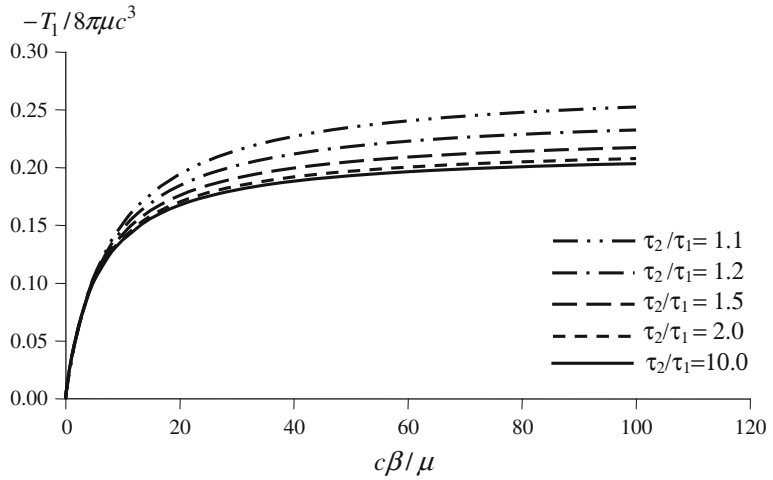

Fig. 3 Normalized torque acting on the prolate spheroid $\xi = \xi_1$ with $\omega_2/\omega_1 = 2$

Table 3 Normalized torque acting on the oblate spheroid $\xi = \xi_1$ with $\lambda_2/\lambda_1 = 2$

ω_2/ω_1	N	$T_1/8\pi\mu\tilde{c}^3\omega_1$				
		$\tilde{c}\beta/\mu = 0.01$	$\tilde{c}\beta/\mu = 0.1$	$\tilde{c}\beta/\mu = 1.0$	$\tilde{c}\beta/\mu = 10.0$	$\tilde{c}\beta/\mu = \infty$
-1.5	10	0.007836	0.077084	0.662009	2.768835	4.314823
	11	0.007836	0.077084	0.662009	2.768835	4.314823
0.0	10	0.003134	0.030834	0.264804	1.107534	1.725929
	11	0.003134	0.030834	0.264804	1.107534	1.725929
1.5	10	−0.001567	−0.015417	−0.132402	−0.553767	−0.862965
	11	−0.001567	−0.015417	−0.132402	−0.553767	−0.862965
2.0	10	−0.003134	−0.030834	−0.264804	−1.107534	−1.725929
	11	−0.003134	−0.030834	−0.264804	−1.107534	−1.725929
5.0	10	−0.012538	−0.123334	−1.059215	−4.430137	−6.903717
	11	−0.012538	−0.123334	−1.059215	−4.430136	−6.903717

Table 4 Normalized couple acting on the oblate spheroid $\xi = \xi_1$ with $\omega_2/\omega_1 = 2$

λ_2/λ_1	N	$T_1/8\pi\mu\tilde{c}^3\omega_1$				
		$\tilde{c}\beta/\mu = 0.01$	$\tilde{c}\beta/\mu = 0.1$	$\tilde{c}\beta/\mu = 1.0$	$\tilde{c}\beta/\mu = 10.0$	$\tilde{c}\beta/\mu = \infty$
1.1	10	−0.002090	−0.020863	−0.202765	−1.726929	−10.837443
	11	−0.002090	−0.020863	−0.202765	−1.726928	−10.837443
1.2	10	−0.002232	−0.022237	−0.213392	−1.587271	−5.717041
	11	−0.002232	−0.022237	−0.213392	−1.587271	−5.717041
1.5	10	−0.002628	−0.026049	−0.238716	−1.318416	−2.683231
	11	−0.002628	−0.026049	−0.238716	−1.318415	−2.683231
2.0	10	−0.003134	−0.030834	−0.264804	−1.107534	−1.725929
	11	−0.003134	−0.030834	−0.264804	−1.107534	−1.725929
10.0	8	−0.003876	−0.037593	−0.288831	−0.876188	−1.137241
	9	−0.003876	−0.037592	−0.288830	−0.876186	−1.137241

in the slip parameter with fixed values of the relative angular velocity and axis ratio for both prolate and oblate spheroidal particles. There is a significant increase in normalized torque for values of the slip parameter less than 10 and tends to a finite value for the classical no-slip case. As expected, the normalized torque becomes zero for perfect slip. It is also observed that when the particle and envelope rotate in opposite directions (i.e., $\omega_2/\omega_1 < 0$), the magnitude of the normalized torque is much greater than that of the corresponding case when the particle and envelope rotate in the same direction)$\omega_2/\omega_1 > 0$) for the different values of axis ratio and slip parameter. Figures 6, and 7 represent the fluid velocity profiles for prolate spheroids versus τ/τ_1 and ζ, respectively, when $c\beta/\mu = 1$ and $\omega_2/\omega_1 = 2$. It can be observed from these two figures that the values of velocity increase monotonically with the increase in the axis ratio and decrease with increase in ζ. For oblate

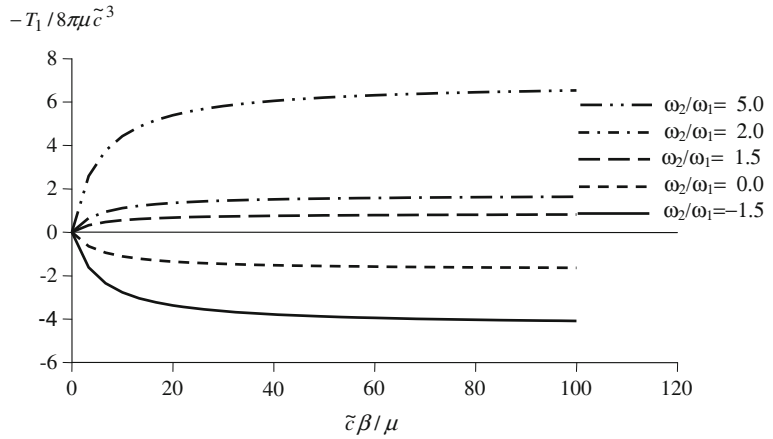

Fig. 4 Normalized torque acting on the oblate spheroid $\xi = \xi_1$ with $\tau_2/\tau_1 = 2$

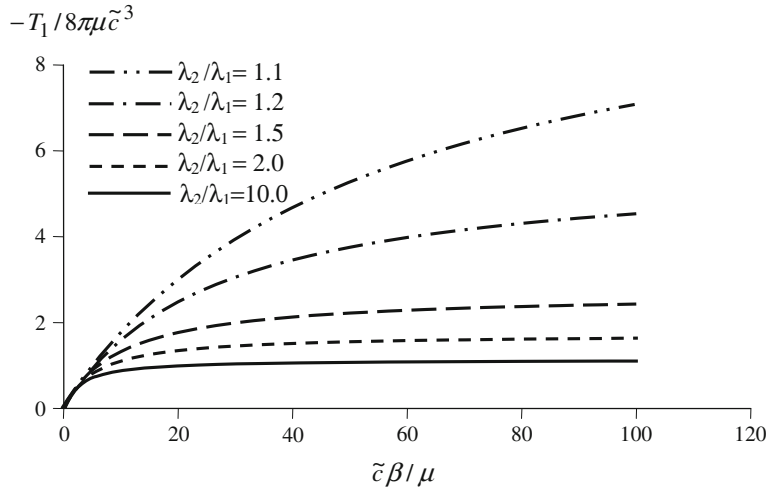

Fig. 5 Normalized torque acting on the oblate spheroid $\xi = \xi_1$ with $\omega_2/\omega_1 = 2$

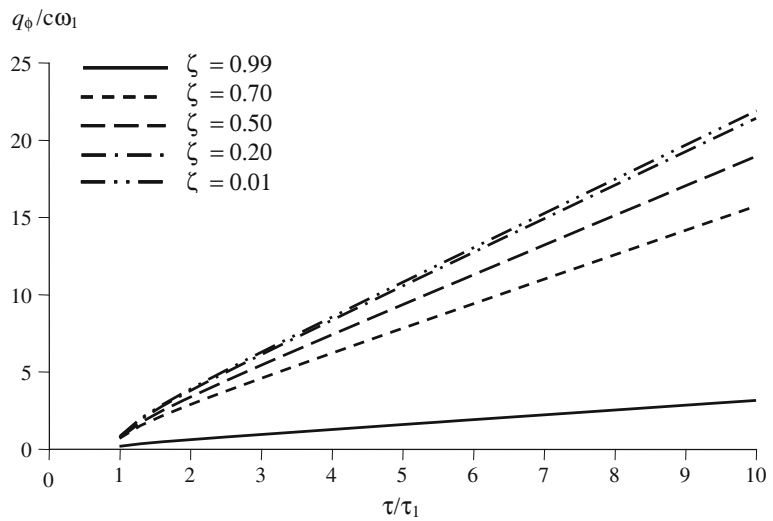

Fig. 6 Velocity profile for prolate spheroids with $c\beta/\mu = 1$, $\omega_2/\omega_1 = 2$

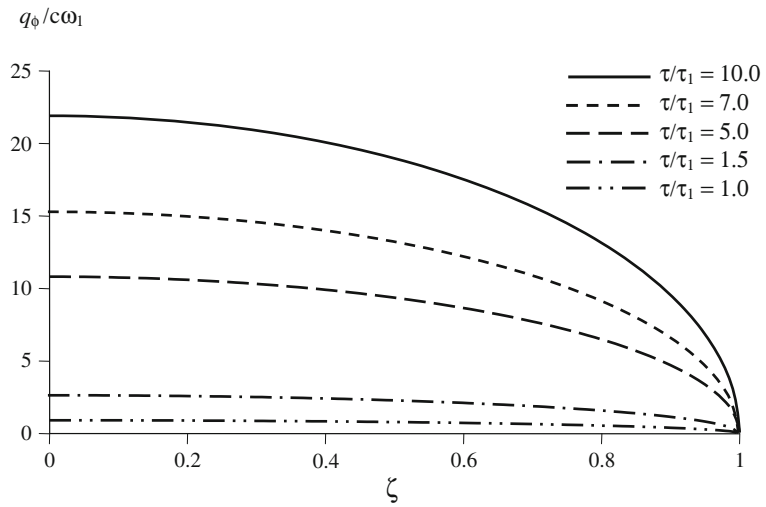

Fig. 7 Velocity profile for prolate spheroids with $c\beta/\mu = 1$, $\omega_2/\omega_1 = 2$

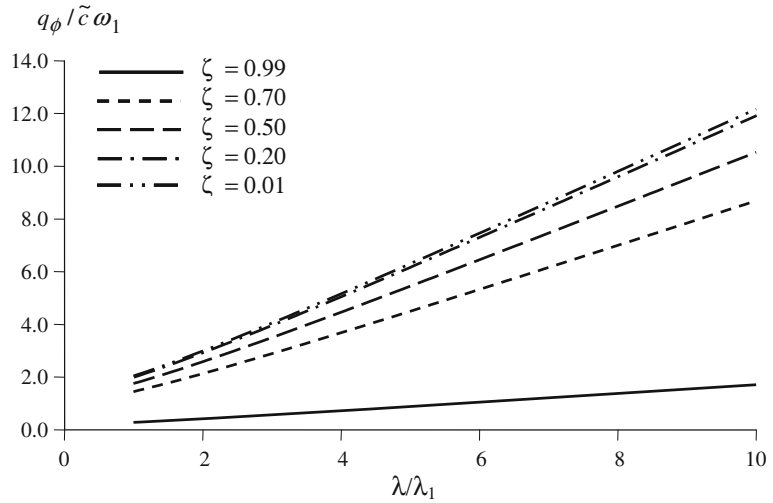

Fig. 8 Velocity profile for oblate spheroids with $\tilde{c}\beta/\mu = 1$, $\omega_2/\omega_1 = 2$

spheroids, the velocity profiles are represented by Figs. 8, and 9 versus $\lambda/\lambda_1$and ζ, respectively. A similar observation to that of Figs. 6, and 7 applies to Figs. 8, and 9.

The solution for oblate spheroids can be obtained by making the following transformations [2]

$$\tau_k \to i\lambda_k \quad \text{and} \quad c \to -i\tilde{c} = -i\sqrt{b_k^2 - a_k^2}, b_k > a_k (k = 1, 2), i = \sqrt{-1}$$

where

$$\lambda = \sinh\xi, \zeta = \cos\eta, 0 \le \lambda < \infty, -1 \le \zeta \le 1.$$

5 Conclusion

In this work, the boundary collocation numerical solution for the hydrodynamic torque acting on a slip spheroidal particle in a container is obtained. The solid particle and the spheroidal container rotate with different angular velocities, in the same or opposite directions, about their axis of revolution. The results for the normalized torque acting on the particle indicate that the solution procedure converges rapidly, and accurate solutions can be obtained for various cases of the particles relative angular velocity, axis ratio, and slip parameter. It has

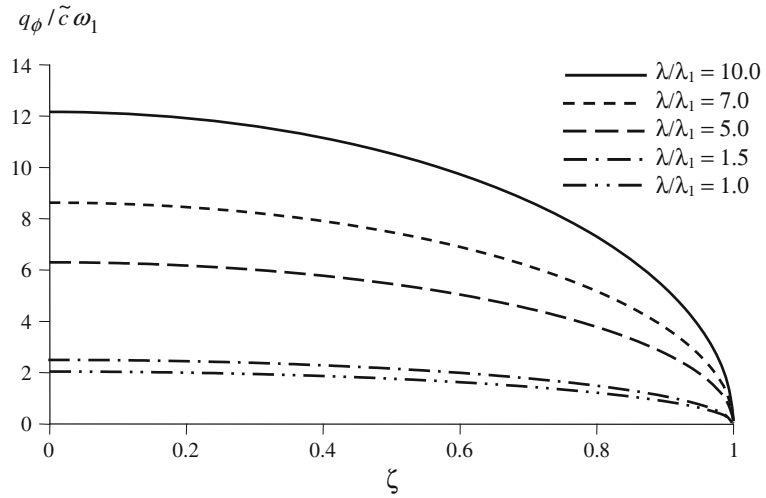

Fig. 9 Velocity profile for oblate spheroids with $\tilde{c}\beta/\mu = 1, \omega_2/\omega_1 = 2$

been found that, for the no-slip of a prolate spheroidal particle in an unbounded fluid ($\tau_2 \to \infty$), our results of the hydrodynamic torque given by (3.18) are in good agreement with those of Jeffery [50].

The normalized torque increases monotonically with the increase in the axis ratio for a fixed relative angular velocity and slip parameter. It also vanishes for perfect slip.

References

1. Keh, H.J., Lee, T.C.: Axisymmetric creeping motion of a slip spherical particle in a nonconcentric spherical cavity. Theor. Comput. Fluid Dyn. **24**, 497–510 (2010)
2. Happel, J., Brenner, H.: Low Reynolds Number Hydrodynamics. Nijho, Dordrecht, The Netherlands (1983)
3. Kim, S., Karrila, S.J.: Microhydrodynamics: Principles and Selected Applications. Butterworth–Heinemann, Boston (1991)
4. Pedlosky, J.: Axially symmetric motion of a stratified, rotating fluid in a spherical annulus of a narrow gape. J. Fluid Mech. **36**, 401–415 (1969)
5. Endo, Y., Kousaka, Y.: Dispersion mechanism of coagulated particles in liquid flow. Colloid. Surf. A **109**, 109–115 (1996)
6. Nakabayashi, K., Tsuchida, Y.: Basic study on classification of fine particles in almost rigidly rotating flow (2nd report, dependence of Ekman layer and interior region on wall configuration of housing and rotor). Trans. Jpn. Soc. Mech. Eng. B **61** (591), 3996–4003 (1995)
7. Nakabayashi, K., Tsuchida, Y., Takeo, K., Ono, Y.: Basic study on classification of fine particles in almost rigidly rotating flow (3rd report, conditions of occurrence of a stable regime of almost rigidly rotating flow). Trans. Jpn. Soc. Mech. Eng. B **61** (591) (1995)
8. Lee, E., Huang, Y.F., Hsu, J.P.: Electrophoresis in a non-Newtonian fluid: sphere in a spherical cavity. J. Colloid Interface Sci. **258**, 283–288 (2003)
9. Lee, E., Ming, J.K., Hsu, J.P.: Purely viscous flow of a shear-thinning fluid between two rotating spheres. Chem. Eng. Sci. **59**, 417–424 (2004)
10. Landau, L.D., Lifshitz, E.M.: Fluid mechanics, volume 6 of course of theoretical physics. Pergamon, New York (1959)
11. Munsun, B.R., Joseph, D.D.: Viscous incompressible flow between concentric rotating sphere, Part 1. Basic Flow. J. Fluid Mech. **49**, 269–303 (1971)
12. Kanwal, R.P.: Slow steady rotation of axially symmetric bodies in a viscous fluid. J. Fluid Mech. **10**, 17–24 (1960)
13. Huh, C., Scriven, L.E.: Hydrodynamic model of steady movement of a solid/liquid/fluid contact line. J. Colloid Interface Sci. **35**, 85–101 (1971)
14. Hocking, L.M.: A moving fluid interface on a rough surface. J. Fluid Mech. **76**, 801–817 (1976)
15. Koplik, J., Banavar, J.R., Willemsen, J.F.: Molecular dynamics of Poiseuille flow and moving contact lines. Phys. Rev. Lett. **60**, 1282–1285 (1988)
16. Thompson, P.A., Robbins, M.O.: Simulations of contact line motion: slip and the dynamic contact angle. Phys. Rev. Lett. **63**, 766–769 (1989)
17. Thompson, P.A., Brinkerhoff, W.B., Robbins, M.O.: Microscopic studies of static and dynamic contact angles. J. Adhesion Sci. Technol. **7**, 535–554 (1993)
18. Moffatt, H.K.: Viscous and resistive eddies near a sharp corner. J. Fluid Mech. **18**, 1–18 (1964)
19. Koplik, J., Banavar, J.R.: Corner flow in the sliding plate problem. Phys. Fluids **7**, 3118–3125 (1995)
20. Pearson, J.R.A., Petrie, C.J.S.: In Wetton, R.E., Whorlow, R.W. (eds.) Polymer Systems: Deformation and Flow, pp. 163–187. Macmillian, London (1968)
21. Richardson, S.: On the no-slip boundary condition. J. Fluid Mech. **59**, 707–719 (1973)

22. Denn, L.M.: Issues in viscoelastic fluid mechanics. Annu. Rev. Fluid Mech. **22**, 13–34 (1990)
23. O'Neill, M.E., Ranger, K.B., Brenner, H.: Slip at the surface of a translating- rotating sphere bisected by a free surface bounding a semi-infinite viscous fluid: removal of the contact-line singularity. Phys. Fluids **29**, 913–924 (1986)
24. Navier, C.L.M.H.: Memoirs de l'Academie Royale des Sciences de l'Institut de France. **1**, 414–416 (1823)
25. Tretheway, D.C., Meinhart, C.D.: Apparent fluid slip at hydrophobic microchannel walls. Phys. Fluids **14**, L9–L12 (2002)
26. Zhu, Y., Granick, S.: Rate-dependent slip of Newtonian liquid at smooth surfaces. Phys. Rev. Lett. **87**, 096105–096108 (2001)
27. Pit, R., Hervet, H., Leger, L.: Direct experimental evidence of slip in hexadecane: solid interfaces. Phys. Rev. Lett. **85**, 980–983 (2000)
28. Choi, C., Westin J., A., Breuer K., S.: Apparent slip flows in hydrophilic and hydrophobic microchannels. Phys. Fluids **15**, 2897–2902 (2003)
29. Neto, C., Evans, D.R., Bonaccurso, E., Butt, H.-J., Craig, V.S.J.: Boundary slip in Newtonian liquids: a review of experimental studies. Rep. Progr. Phys. **68**, 2859–2897 (2005)
30. Willmott, G.: Dynamics of a sphere with inhomogeneous slip boundary conditions in Stokes flow. Phys. Rev. E **77**, 055302–055314 (2008)
31. Suna, H., Liu, C.: The slip boundary condition in the dynamics of solid particles immersed in Stokesian flows. Solid State Commun. **150**, 990–1002 (2010)
32. Zhang, H., Zhang, Z., Zheng, Y., Ye, H.: Corrected second-order slip boundary condition for fluid flows in nanochannels. Phys. Rev. E **81**, 066303–066316 (2010)
33. Yang, F.: Slip boundary condition for viscous flow over solid surfaces. Chem. Eng. Comm. **197**, 544–550 (2010)
34. Whitmer, J.K., Luijten, E.: Fluid-solid boundary conditions for multiparticle collision dynamics. J. Phys. Condens. Matter **22**, 104106 (2010)
35. Sherief, H.H., Faltas, M.S., Saad, E.I.: Slip at the surface of a sphere translating perpendicular to a plane wall in micropolar fluid. ZAMP **59**, 293–312 (2008)
36. Sherief, H.H., Faltas, M.S., Ashmawy, E.A.: Galerkin representations and fundamental solutions for an axisymmetric microstretch fluid flow. J. Fluid Mech. **619**, 277–293 (2009)
37. Loyalka, S.K., Griffin, J.L.: Rotation of non-spherical axi-symmetric particles in the slip regime. J. Aerosol Sci. **25**, 509–525 (1994)
38. Williams, M.M.R., Loyalka, S.K.: Aerosol Science: Theory and Practice. Pergamon, New York (1991)
39. Chang, Y.C., Keh, H.J.: Creeping-flow rotation of a slip spheroid about its axis of revolution. Theor. Comput. Fluid Dyn. (2010). doi:10.1007/s00162-010-0216-4
40. Ashmawy, E.A.: Slip at the surface of a general axi-symmetric body rotating in a viscous fluid.. Arch. Mech. **63**, 1–21 (2011)
41. Gluckman, M.J., Pfeffer, R., Weinbaum, S.: A new technique for treating multiparticle slow viscous flow: axisymmetric flow past spheres and spheroids. J. Math. Mech. **50**, 705–740 (1971)
42. Leichtberg, S., Pfeffer, R., Weinbaum, S.: Stokes flow past finite coaxial clusters of spheres in a circular cylinder. Int. J. Multiphase Flow **3**, 147–169 (1976)
43. Ganatos, P., Weinbaum, S., Pfeffer, R.: A strong interaction theory for the creeping motion of a sphere between plane parallel boundaries. Part 1. Perpendicular motion.. J. Fluid Mech. **99**, 739–753 (1980)
44. Ganatos, P., Weinbaum, S., Pfeffer, R.: A strong interaction theory for the creeping motion of a sphere between plane parallel boundaries. Part 2. Parallel motion.. J. Fluid Mech. **99**, 755–783 (1980)
45. Lu, S.Y., Lee, C.T.: Boundary effects on creeping motion of an aerosol particle in a nonconcentric pore. Chem. Eng. Sci. **56**, 5207–5216 (2001)
46. Chen, P.Y., Keh, H.J.: Slow motion of a slip spherical particle parallel to one or two plane walls. J. Chin. Inst. Chem. Eng. **34**, 123–133 (2003)
47. Lu, S.Y., Lee, C.T.: Creeping motion of a spherical aerosol particle in a cylindrical pore. Chem. Eng. Sci. **57**, 1479–1484 (2002)
48. Sherief, H.H., Faltas, M.S., Ashmawy, E.A.: Slow motion of a sphere moving normal to two infinite parallel plane walls in a micropolar fluid. Math. Comput. Model. **53**, 376–386 (2011)
49. Basset, A.B.: A Treatise on Hydrodynamics, vol. 2. Dover, New York (1961)
50. Jeffery, G.B.: On the steady rotation of a solid of revolution in a viscous fluid. Proc. Lond. Math. Soc. **14**, 327–338 (1915)